Asian Journal of Chemistry; Vol. 35, No. 12 (2023), 2963-2970

ASIAN JOURNAL OF CHEMISTRY

https://doi.org/10.14233/ajchem.2023.29062

Evaluation of Cytotoxicity of 1*H*-1,2,4-Triazole-3-carboxamide Derivatives in Various Cancer Cell Lines using MTT Assay: Synthesis, Characterization and Molecular Docking Studies

DIPESH KUMAR SHARMA and SURABHI SINGH*

School of Basic and Applied Sciences, Career Point University, Kota-325003, India

*Corresponding author: E-mail: surabhisinghcpu@gmail.com

Received: 14 August 2023; *Accepted*: 18 October 2023; *Published online*: 2 December 2023; AJC-21456

The pursuit of discovering efficacious novel anticancer agents is an ongoing and perpetual endeavour. The ongoing research endeavour involves the discovery of a new set of various substituted 1,2,4-triazole carboxamide derivatives. The synthetic process involves multiple steps: converting thiooxamic acid ethyl ester to ethyl β-N-boc-oxalamidrazone (**2**), preparing ethyl esters of 5-substituted 1,2,4-triazole-3-carboxylic acid (**3**) and synthesizing 5-substituted 1,2,4-triazole-3-carboxylic acid amides (**4a-n**) using potassium *tert.*-butoxide. The resulting compounds are characterized using ^{1}H and ^{13}C NMR spectroscopy and HRMS. Molecular docking experiments were performed using the synthesized compounds against two cancer targets, *viz.* EGFR (6LUD) and CDK-4 (7SJ3). The compounds were assessed for their anticancer potential against four different cancer cell lines, namely non-small cell lung cancer (A-549), pancreatic cancer (PANC-1), colorectal cancer (HCT-116) and cervical cancer (HaLa) cell lines. Additionally, a normal human embryonic kidney cell line (HEK-293) was used for comparison. The results obtained from molecular docking analysis demonstrated that the 1,2,4-triazole carboxamides (**4c**, **4e**, **4h**, **4m** and **4n**) exhibited more favourable binding interactions compared to the ligands that were co-crystallized. All the compounds exhibited a satisfactory cytotoxicity profile in comparison to the reference drug doxorubicin. Among the compounds that tested, it was observed that compounds **4e** and **4m** displayed the most pronounced inhibitory activity across all the cell lines that were tested.

Keywords: 1,2,4-Triazole, Anticancer, MTT assay, EGFR, CDK-4.

INTRODUCTION

Cancer, a complex and formidable group of diseases, presents a global health challenge due to its uncontrolled cell growth and potential life-threatening consequences [1]. Chemotherapy, a widely used and time-tested approach, employs potent drugs to target and eliminate rapidly dividing cancer cells throughout the body. Though effective, chemotherapy may cause side effects by affecting normal cells. The imperative development of novel anticancer agents stems from the potential side effects of chemotherapy on normal cells [2]. While effective against cancer cells, chemotherapy's non-specific nature causes collateral damage to healthy tissues, leading to adverse reactions impacting a patient's quality of life and treatment efficacy. Targeted therapies aim to selectively attack cancer cells while sparing healthy tissues, reducing side effects and enhancing treatment precision [3].

1,2,4-Triazole scaffold has emerged as a versatile and promising building block in the development of novel anticancer agents. Its structural diversity allows for the introduction of various substituents, enabling the design of compounds with improved properties [4]. The triazole ring acts as a bio-isostere, replacing conventional moieties in medicinal chemistry [5].

The significance of 1,2,4-triazole scaffold is emphasized by the efficacy and extensive utilization of pharmaceuticals such as anastrozole and letrozole for managing hormone receptor-positive breast cancer [6]. The inhibitory effects of 1,2,4-triazole derivatives on a range of cancer-related targets, such as EGFR [7], VEGFR [8-10], thymidine phosphorylase [11,12], topoisomerase [13,14], aromatase [15] and tubulin polymerization [16,17] have been emphasized in recent reports.

The aforementioned findings indicate the potential of these therapies to specifically target and disrupt key pathways that play a crucial role in the proliferation of cancer cells. Additionally, they can overcome drug resistance, a major challenge in cancer treatment [18]. Certain derivatives have favourable pharmacokinetic profiles, contributing to their potential as

clinically viable anticancer agents [19]. Overall, 1,2,4-triazole scaffold holds great promise in advancing cancer treatment and improving patient outcomes.

In light of the structural diversity and ability to interact multiple targets, along with the advantageous pharmacokinetic characteristics, we embarked upon the synthesis and assessment of novel derivatives based on the 1,2,4-triazole scaffold, with the aim of investigating their potential as anticancer agents. Moreover, the study involved the utilization of molecular docking techniques to investigate the molecular interactions between the designed derivatives and EGFR, CDK-4 targets, aiming to gain insights into the potential underlying mechanism.

EXPERIMENTAL

No additional purification steps were taken on any of the synthetic-grade compounds or solvents that were utilized in this investigation were all procured from Sigma-Aldrich, India. For the reaction monitoring, Merck-precoated aluminium TLC plates coated with silica gel 60 F_{254} were utilized. Remi electronic melting point equipment was used to make the determination of the melting points. The ^{1}H & ^{13}C NMR spectra were acquired using a BRUKER DRX instrument and the chemical shift values, which were reported in ppm, were relative to the internal standard, which was tetramethyl silane. The HRMS spectra were obtained by employing a Waters Xevo Q-Tof Mass spectrometer in their collection.

Synthesis of ethyl β-N-Boc-oxalamidrazone (2): Both thiooxamic acid ethyl ester (**1**) (18.23 g, 137 mmol) and Boc-hydrazine (18.10 g, 137 mmol) were dissolved in EtOH (80 mL) in a single necked round-bottomed flask. A white precipitate was produced after stirring the reaction mixture for 24 h. After being filtered off, precipitate of ethyl β-N-Boc-oxalamidrazone (**2**) that had formed was then washed with 10 mL of EtOH and air-dried [20].

Synthesis of ethyl esters of 5-substituted 1,2,4-triazole-3-carboxylic acid (3): A suspension containing ethyl β-N-Boc-oxalamidrazone (**2**) in 10 mL of toluene was placed within a single-necked round-bottom flask. Subsequently, anhydrous pyridine (3 equiv.) was introduced, followed by a gradual addition of acetyl chloride (2 equiv.). The resulting reaction mixture was subjected to reflux for a duration of 12 h, with the progression of the reaction being monitored using thin-layer chromatography (TLC). Upon attainment of reaction completion, the solvent was eliminated *via* rotary evaporation. The resultant reaction mixture was quenched with water and subjected to extraction with three equilibrated portions (3 × 15 mL) of ethyl acetate. The consolidated organic phases were subjected to desiccation using anhydrous Na_2SO_4, followed by subsequent solvent removal through rotary evaporation. The final product, comprising ethyl esters of 5-substituted 1,2,4-triazole-3-carboxylic acid (**3**), was isolated using column chromatography on silica gel. This purification process employed a mobile phase consisting of a 10% ethyl acetate-hexane solvent system [20].

Synthesis of 5-substituted 1,2,4-triazole-3-carboxamides (4a-n): A solution of 6.6 mmol of potassium *tert*-butoxide (KOt-Bu) was prepared by dissolving it in 40 mL of THF under stirring in ambient air at room temperature for a duration of 1 min. Subsequently, a mixture comprising 3.3 mmol of ethyl esters of 5-substituted 1,2,4-triazole-3-carboxylic acid (**3**) and 3.3 mmol of various substituted aryl amines (**4a-n**) was promptly added to the solution. The resultant mixture was stirred at room temperature until the arylamine was completely consumed in the reaction. Following this, THF solvent was removed under reduced pressure. To the residue, 50 mL of water was introduced and subsequent extraction with dichloromethane was performed. The organic layer was separated and subjected to drying using anhydrous sodium sulfate. Evaporation of the solvent under reduced pressure led to the isolation of the corresponding 5-substituted 1,2,4-triazole-3-carboxamides (**4a-n**) (**Scheme-I**). The purification of these products was achieved through column chromatography using an ethyl acetate-*n*-hexane (1:4) solvent system as mobile phase [21].

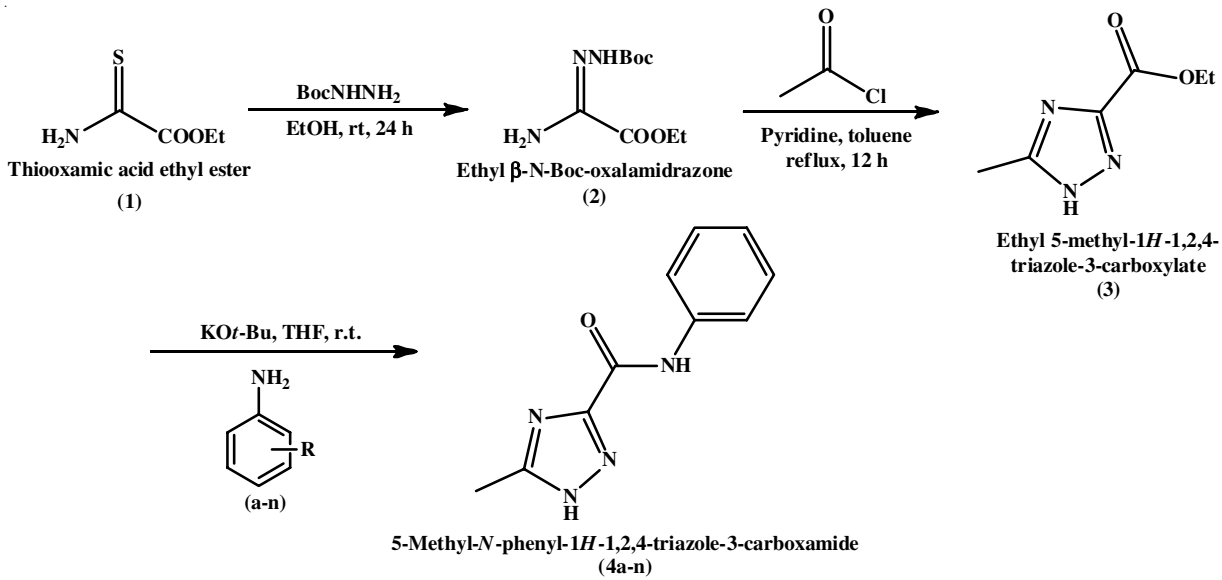

Scheme-I: Scheme of synthesis for the 1,2,4-triazole carboxamide derivatives

5-Methyl-N-phenyl-1*H*-1,2,4-triazole-3-carboxamide (4a): Off white solid, yield: 69%, m.p.: 196-198 ºC; ^{1}H NMR (500 MHz, DMSO-d_6) δ ppm: 13.43 (s, 1H), 9.03 (s, 1H), 7.71-7.65 (m, 2H), 7.36-7.29 (m, 2H), 7.03 (tt, *J* = 6.9, 1.1 Hz, 1H), 2.51 (s, 3H). ^{13}C NMR (125 MHz, DMSO-d_6) δ ppm: 157.36, 155.32, 152.11, 137.62, 128.77, 123.80, 120.84, 13.44. HRMS: *m/z* for $C_{10}H_{10}N_4O$ ([M + H]$^+$): 203.0515, found 203.0518.

5-Methyl-N-(*m*-tolyl)-1*H*-1,2,4-triazole-3-carboxamide (4b): Off white solid, yield: 72%, m.p.: 174-175 ºC; ^{1}H NMR (500 MHz, DMSO-d_6) δ ppm: 13.51 (s, 1H), 8.92 (s, 1H), 7.46-7.38 (m, 2H), 7.18 (t, *J* = 7.7 Hz, 1H), 6.94 (ddt, *J* = 7.6, 1.6, 0.8 Hz, 1H), 2.38 (s, 3H), 2.22 (s, 2H). ^{13}C NMR (125 MHz, DMSO-d_6) δ ppm: 158.48, 156.74, 150.94, 138.74, 138.06, 129.71, 124.85, 121.44, 117.82, 21.92, 13.44. HRMS: *m/z* for $C_{11}H_{12}N_4O$ ([M + H]$^+$): 217.1017, found 217.1011.

5-Methyl-N-(*p*-tolyl)-1*H*-1,2,4-triazole-3-carboxamide (4c): Off white solid, Yield: 70%, m.p.: 181-182 ºC, ^{1}H NMR (500 MHz, DMSO-d_6) δ 13.46 (s, 1H), 8.79 (s, 1H), 7.48-7.42 (m, 2H), 7.27 (dd, *J* = 8.5, 1.0 Hz, 2H), 2.46 (s, 3H), 2.27 (d, *J* = 1.1 Hz, 2H). ^{13}C NMR (125 MHz, DMSO-d_6) δ ppm: 158.48, 154.35, 150.94, 137.03, 133.11, 128.77, 119.99, 21.70, 13.66. HRMS: *m/z*: For $C_{11}H_{12}N_4O$ ([M + H]$^+$): 217.1108, found 217.1105.

***N*-(4-Methoxyphenyl)-5-methyl-1*H*-1,2,4-triazole-3-carboxamide (4d):** Off white solid, yield: 71%, m.p.: 190-191 ºC; ^{1}H NMR (500 MHz, DMSO-d_6) δ ppm: 13.63 (s, 1H), 9.21 (s, 1H), 7.59-7.53 (m, 2H), 6.96-6.90 (m, 2H), 3.73 (s, 3H), 2.51 (s, 3H). ^{13}C NMR (125 MHz, DMSO-d_6) δ ppm: 58.48, 157.76, 155.32, 152.07, 131.66, 121.23, 115.14, 54.03, 11.92. HRMS: *m/z* for $C_{11}H_{12}N_4O_2$ ([M + H]$^+$): 233.0938, found 233.0931.

***N*-(2-Aminophenyl)-5-methyl-1*H*-1,2,4-triazole-3-carboxamide (4e):** Off white solid, yield: 67%, m.p.: 203-204 ºC; ^{1}H NMR (500 MHz, DMSO-d_6) δ ppm: 13.52 (s, 1H), 9.35 (s, 1H), 7.60 (dd, *J* = 7.8, 1.4 Hz, 1H), 7.34-7.27 (m, 1H), 6.96 (td, *J* = 7.5, 1.3 Hz, 1H), 6.88 (dd, *J* = 8.0, 1.3 Hz, 1H), 4.76 (s, 2H), 2.51 (s, 3H). ^{13}C NMR (125 MHz, DMSO-d_6) δ ppm: 156.74, 154.06, 150.94, 139.93, 130.00, 123.40, 121.01, 120.50, 114.20, 11.92. HRMS: *m/z* for $C_{10}H_{11}N_5O$ ([M + H]$^+$): 218.1527, found 218.1527.

***N*-(4-Aminophenyl)-5-methyl-1*H*-1,2,4-triazole-3-carboxamide (4f):** Pale yellow solid, yield: 69%, m.p.: 209-210 ºC; ^{1}H NMR (500 MHz, DMSO-d_6) δ ppm: 13.55 (s, 1H), 9.45 (s, 1H), 7.50-7.44 (m, 2H), 6.64-6.58 (m, 2H), 5.10 (s, 2H), 2.48 (s, 3H). ^{13}C NMR (125 MHz, DMSO-d_6) δ ppm: 158.92, 156.96, 153.55, 145.07, 133.11, 122.00, 115.45, 12.93. HRMS: *m/z* for $C_{10}H_{11}N_5O$ ([M + H]$^+$): 218.1530, found 218.1526.

***N*-(4-Hydroxyphenyl)-5-methyl-1*H*-1,2,4-triazole-3-carboxamide (4g):** Off white solid, yield: 68%, m.p.: 216-217 ºC; ^{1}H NMR (500 MHz, DMSO-d_6) δ ppm: 13.63 (s, 1H), 9.47 (s, 1H), 8.78 (s, 1H), 7.34-7.28 (m, 2H), 6.79-6.72 (m, 2H), 2.41 (s, 3H). ^{13}C NMR (125 MHz, DMSO-d_6) δ ppm: 159.43, 156.74, 154.79, 152.83, 133.11, 121.44, 114.92, 12.93. HRMS: *m/z* for $C_{10}H_{10}N_4O_2$ ([M + H]$^+$): 219.0944, found 219.0494.

***N*-(4-Fluorophenyl)-5-methyl-1*H*-1,2,4-triazole-3-carboxamide (4h):** Light brown solid, yield: 76%, m.p.: 209-210 ºC; ^{1}H NMR (500 MHz, DMSO-d_6) δ ppm: 13.28 (s, 1H), 8.97 (s, 1H), 7.58-7.51 (m, 2H), 7.18-7.10 (m, 2H), 2.48 (s, 3H). ^{13}C NMR (125 MHz, DMSO-d_6) δ ppm: 157.23 (d, *J* = 5.5 Hz), 154.06, 150.94, 135.80 (d, *J* = 2.9 Hz), 123.40 (d, *J* = 8.7 Hz), 116.03, 115.85, 13.44. HRMS: *m/z* for $C_{10}H_9FN_4O$ ([M + H]$^+$): 221.0785, found 221.0785.

***N*-(4-Chlorophenyl)-5-methyl-1*H*-1,2,4-triazole-3-carboxamide (4i):** Off white solid, yield: 78%, m.p.: 221-222 ºC; ^{1}H NMR (500 MHz, DMSO-d_6) δ ppm: 13.51 (s, 1H), 9.10 (s, 1H), 7.65-7.59 (m, 2H), 7.42-7.36 (m, 2H), 2.51 (s, 3H). ^{13}C NMR (125 MHz, DMSO-d_6) δ ppm: 156.74, 155.32, 152.11, 137.25, 128.26, 126.81, 120.50, 12.93. HRMS: *m/z* for $C_{10}H_9ClN_4O$ ([M + H]$^+$): 236.0536, found 236.0531.

***N*-(4-Bromophenyl)-5-methyl-1*H*-1,2,4-triazole-3-carboxamide (4j):** Light brown solid, yield: 71%, m.p.: 198-199 ºC; ^{1}H NMR (500 MHz, DMSO-d_6) δ ppm: 13.49 (s, 1H), 9.24 (s, 1H), 7.62-7.56 (m, 2H), 7.52-7.46 (m, 2H), 2.54 (s, 3H). ^{13}C NMR (125 MHz, DMSO-d_6) δ ppm: 157.33, 155.32, 152.11, 136.80, 132.87, 123.77, 118.94, 12.49. HRMS: *m/z* for $C_{10}H_9BrN_4O$ ([M + H]$^+$): 282.0522, found 282.0522.

5-Methyl-N-(4-(trifluoromethyl)phenyl)-1*H*-1,2,4-triazole-3-carboxamide (4k): Off white solid, yield: 77%, m.p.: 185-186 ºC; ^{1}H NMR (500 MHz, DMSO-d_6) δ ppm: 13.67 (s, 1H), 9.51 (s, 1H), 7.88-7.82 (m, 2H), 7.81-7.76 (m, 1H), 7.76-7.70 (m, 1H), 2.38 (s, 3H). ^{13}C NMR (125 MHz, DMSO-d_6) δ 157.36, 155.32, 152.11, 138.02, 126.71 (q, *J* = 4.6 Hz), 120.22 (q, *J* = 3.7 Hz), 13.15. HRMS: *m/z* for $C_{11}H_9F_3N_4O$ ([M + H]$^+$): 271.0728, found 271.0725.

***N*-(2,4-Dichlorophenyl)-5-methyl-1*H*-1,2,4-triazole-3-carboxamide (4l):** Off white solid, yield: 75%, m.p.: 171-172 ºC; ^{1}H NMR (500 MHz, DMSO-d_6) δ ppm: 13.45 (s, 1H), 9.45 (s, 1H), 7.72-7.66 (m, 2H), 7.37 (dd, *J* = 8.2, 2.3 Hz, 1H), 2.35 (s, 3H). ^{13}C NMR (125 MHz, DMSO-d_6) δ ppm: 157.98, 155.32, 151.96, 136.73, 129.16, 128.57, 128.04, 127.50, 124.32, 11.70. HRMS: *m/z* for $C_{10}H_8Cl_2N_4O$ ([M + H]$^+$): 272.0164, found 272.0162.

5-Methyl-N-(3-nitrophenyl)-1*H*-1,2,4-triazole-3-carboxamide (4m): Pale yellow solid, yield: 66%, m.p.: 157-158 ºC; ^{1}H NMR (500 MHz, DMSO-d_6) δ ppm: 13.51 (s, 1H), 9.82 (s, 1H), 8.67 (t, *J* = 2.3 Hz, 1H), 8.05 (ddd, *J* = 8.0, 2.3, 1.1 Hz, 1H), 7.78 (ddd, *J* = 8.0, 2.2, 1.3 Hz, 1H), 7.62 (t, *J* = 7.9 Hz, 1H), 2.45 (s, 3H). ^{13}C NMR (125 MHz, DMSO-d_6) δ ppm: 157.27, 155.32, 152.11, 148.64, 139.20, 130.65, 126.85, 117.62, 114.96, 12.49. HRMS: *m/z* for $C_{10}H_9N_5O_3$ ([M + H]$^+$): 248.0695, found 248.0691.

5-Methyl-N-(4-nitrophenyl)-1*H*-1,2,4-triazole-3-carboxamide (4n): Pale yellow solid, Yield: 68%, m.p.: 159-161 °C, ^{1}H NMR (500 MHz, DMSO-d_6) δ 13.54 (s, 1H), 9.99 (s, 1H), 8.31 (tt, *J* = 7.1, 1.1 Hz, 2H), 7.90-7.84 (m, 2H), 2.51 (s, 3H). ^{13}C NMR (125 MHz, DMSO-d_6) δ ppm: 157.41, 155.32, 152.07, 143.47, 141.74, 125.46, 118.81, 12.49. HRMS: *m/z*: For $C_{10}H_9N_5O_3$ ([M + H]$^+$): 248.0696, found 248.0691.

Molecular docking: The protein data bank provided EGFR (6LUD) and two CDK-4 (7SJ3) domain X-ray crystal structures. The protein preparation wizard feature in Schrödinger software added hydrogen atoms and allocated bond orders in the protein's 3D structure. The LigPrep module in Schrödinger software prepared chiral ligands and optimized their 3D structures using

the OPLS 2005 force field. The SITEMAP ANALYSIS TOOL of Maestro 11.8 was used to analyze receptor sites for 6LUD and 7SJ3, followed by Schrödinger suite's grid creation tool. The XP glide score was derived using binding interaction energy, van der Waals energy, electrostatic potential energy and strain energy assessments during molecular docking using Glide's extra-precision docking modes (Glide XP). The Schrödinger maestro interface was used to study ligand binding to EGFR and CDK-4 active sites [22].

MTT assay: The cytotoxicity and cell viability of 1*H*-1,2,4-triazole-3-carboxamide derivatives (**4a-n**) was MTT assay evaluated. Human cancer cell lines (A-549, HCT-116, PANC-1, HaLa) and a normal cell line (HEK-293) were cultured in 96-well plates, exposed to varying concentrations (0.1 µM, 10 µM, 50 µM and 100 µM) of derivatives for 24-72 h. After incubation, MTT solution induced formazan crystal formation, solubilized with DMSO and absorbance was measured using a microplate reader. The correlation between absorbance values and cell viability was examined, with lower absorbance values indicating greater cytotoxicity and decreased cell viability. The data collected from the MTT assay at various concentrations and time intervals were examined in order to ascertain the half-maximal inhibitory concentration (IC_{50}) values of 1*H*-1,2,4-triazole-3-carboxamide derivatives for each individual cell line. The experiments were conducted in triplicate, with the inclusion of appropriate controls to verify the accuracy and reliability of the assay [23].

RESULTS AND DISCUSSION

Three-step synthesis of 5-substituted 1,2,4-triazole-3-carboxylic acid amides successfully yielded the compounds with moderate to good yields. The process involves converting thiooxamic acid ethyl ester to ethyl β-N-Boc-oxalamidrazone (**2**) in ethanol. This likely proceeds *via* hydrazine nitrogen's nucleophilic attack on thioamide carbon, followed by thiolate anion elimination. The second step cyclizes ethyl β-N-Boc-oxalamidrazone into 1,2,4-triazole using acetyl chloride. The final step converts ethyl esters of 5-substituted 1,2,4-triazole-3-carboxylic acid (**3**) to 5-substituted 1,2,4-triazole-3-carboxamides (**4a-n**). Ethyl esters react with concentrated arylamines in THF at room temperature using KOt-Bu catalyst, forming the desired amides. The ^{1}H NMR data for all the compounds displayed distinct chemical shifts, particularly the singlet peaks corresponding to the N-H signals of the carboxamide and triazole ring N-H. These peaks were observed in the range of 8.8-9.3 and 13.2-13.8 ppm, respectively. Moreover, in the ^{13}C spectrum of all compounds, the carbonyl carbon of carboxamide linkage was observed in the range of approximately 151 to 160 ppm. This observation indicates the successful formation of carboxamide linkage between the triazole and arylamine components. Each of the newly synthesized compounds exhibited respective *m/z* ($M+H^+$) peaks in the high-resolution mass spectrum (HRMS).

Molecular docking studies: Table-1 presents the data of various 1,2,4-triazole carboxamide derivatives (**4a-n**) and their docking scores with targets EGFR (6LUD) and CDK-4 (7SJ3). Each compound was characterized by different substituent group attached to the aryl ring of 1,2,4-triazole carboxamide core. The docking scores represent the strength of interaction between the derivatives and targets EGFR and CDK-4, with lower scores indicating stronger binding affinity.

Molecular docking results of 1,2,4-triazole carboxamide derivatives with 6LUD: 1,2,4-Triazole carboxamide derivatives (**4a-n**) encompassing various substituent groups (-H, $-CH_3$, $-OCH_3$, $-NH_2$, -OH, -F, -Cl, -Br, $-CF_3$, $-NO_2$) exhibit docking scores within the approximate range of -4.7 to -6.3. The ligand osimertinib, which has formed a co-crystal with EGFR, exhibits a docking score of -5.952. The observed score bears resemb-

TABLE-1
RESULTS OF MOLECULAR DOCKING STUDIES AND MTT ASSAY OF SYNTHESIZED 1,2,4-TRIAZOLE CARBOXAMIDE DERIVATIVES (**4a-n**)

Compound	R	Docking scores		IC_{50} values (µM)				
		EGFR (6LUD)	CDK-4 (7SJ3)	Non-small cell lung cancer line (A-549)	Colorectal cancer cell line (HCT-116)	Pancreatic cancer cell line (PANC-1)	Cervical cancer cell line (HaLa)	Human embryonic kidney cell line (HEK-293)
4a	-H	-5.341	-7.061	18.52 ± 2.18	18.71 ± 1.56	28.92 ± 2.78	18.8 ± 3.36	44.6 ± 1.22
4b	-3-CH_3	-5.494	-7.317	25.23 ± 1.58	21.05 ± 3.39	20.36 ± 3.74	23.64 ± 2.94	41.25 ± 1.85
4c	-4-CH_3	-5.362	-7.634	12.36 ± 0.97	14.21 ± 1.37	15.66 ± 1.95	14.08 ± 2.25	39.17 ± 5.2
4d	-4-OCH_3	-6.258	-7.391	14.76 ± 2.24	12.61 ± 1.13	15.32 ± 1.13	15.97 ± 1.14	37.25 ± 2.31
4e	-2-NH_2	-5.699	-8.478	7.11 ± 1.12	5.11 ± 1.88	12.38 ± 4.3	10.39 ± 1.88	32.17 ± 5.2
4f	-4-NH_2	-5.833	-6.965	19.75 ± 1.23	17.22 ± 2.23	19.51 ± 1.19	20.08 ± 1.34	37.95 ± 2.81
4g	-4-OH	-5.908	-7.368	18.01 ± 1.12	19.6 ± 1.25	19.40 ± 2.87	166.02 ± 2.12	37.68 ± 1.44
4h	-4-F	-5.191	-7.644	10 ± 1.18	16.71 ± 1.36	8.32 ± 2.18	11.8 ± 1.32	40.39 ± 1.3
4i	-4-Cl	-4.727	-7.476	21.34 ± 3.58	24.61 ± 2.39	31.72 ± 3.83	24.73 ± 4.33	44.25 ± 1.8
4j	-4-Br	-4.823	-7.337	21.72 ± 2.18	19.87 ± 1.56	28.97 ± 1.28	20.84 ± 1.38	44.6 ± 1.04
4k	-4-CF_3	-5.415	-7.133	26.45 ± 2.74	18.05 ± 3.39	20.72 ± 3.83	22.37 ± 2.4	39.62 ± 1.8
4l	-2,4-Cl	-5.131	-7.326	22.77 ± 4.18	19.01 ± 1.26	27.93 ± 1.78	23.1 ± 3.32	35.36 ± 3.7
4m	-3-NO_2	-5.995	-7.209	6.97 ± 1.12	10.6 ± 1.25	14.84 ± 2.87	6.42 ± 1.97	31.52 ± 3.5
4n	-4-NO_2	-6.316	-7.203	10.51 ± 2.18	12.71 ± 1.82	16.94 ± 2.78	14.78 ± 3.36	40.93 ± 1.51
Osimertinib		-5.952	–	–	–	–	–	–
Abemaciclib		–	-7.541	–	–	–	–	–
Doxorubicin		–	–	1.05 ± 0.95	2.39 ± 0.92	1.84 ± 0.81	1.93 ± 1.28	2.94 ± 1.05

lance to the docking scores of certain compounds listed in the table, indicating that certain derivatives of 1,2,4-triazole carboxamide may possess the ability to interact with EGFR in a manner akin to Osimertinib. Upon comparing the docking scores of the compounds, it is evident that the inclusion of specific substituents, namely -4-NO_2 (-6.316) and -4-OCH_3 (-6.258), leads to elevated docking scores. This observation suggests that these substituents foster more robust interactions with the EGFR. In contrast, the docking scores of -4-Cl (-4.727) and -4-Br (-4.823) are comparatively lower, indicating less robust interactions. These observations suggest that specific substituents have the potential to either increase or decrease the binding affinity of the 1,2,4-triazole carboxamide derivatives for EGFR. The substituent 4-NH_2 (-5.833) exhibits a elevated docking score, suggesting a robust interaction with EGFR. This finding holds significance in the context of refining the compound for potential drug development. The molecular interactions of the compounds with higher docking scores against EGFR *viz.* **4n** and **4m** were displayed in Fig. 1a.

The docking scores indicate that specific substituents, namely -4-NO_2, -4-OCH_3, -4-NH_2, -OH, -CF_3 and -2,4-Cl, exhibit enhanced interactions with EGFR, thereby contributing to stronger binding. Conversely, substituents such as -Cl and -Br lead to diminished interactions, resulting in weaker binding. The binding affinity of 1,2,4-triazole carboxamide derivatives with EGFR is significantly influenced by the chemical nature and position of the substituent groups on the aryl ring.

Molecular docking results of 1,2,4-triazole carboxamide derivatives with 7SJ3: Among the substituent groups, the presence of a simple hydrogen atom (**4a**, -7.061) results in a moderate docking score, suggesting a moderate interaction with CDK-4. The addition of methyl group (**4b**, -7.317) slightly weakens the binding affinity, while a methyl group at a different position (**4c**, -7.634) further decreases the docking score, indicating positional effects on the interaction. The introduction of a methoxy group (**4d**, -7.391) significantly enhances the docking score, suggesting a stronger interaction with CDK-4. Remarkably, the presence of an amino group (**4e**, -8.478) leads to the highest docking score among all compounds, indicating a considerably strong interaction with CDK-4.

The position of amino group (**4f**, -6.965) influences the binding affinity, as it exhibits a lower docking score compared to **4e**. A hydroxyl group (**4g**, -7.368) contributes to a strong docking score, while a fluorine atom (**4h**, -7.644) results in a stronger interaction with CDK-4 compared to a hydrogen atom. A chlorine atom (**4i**, -7.476) at the appropriate position also leads to a relatively high docking score, suggesting a favourable interaction. Similarly, bromine atom (**4j**, -7.337) shows a relatively high docking score, indicating a favourable interaction with CDK-4.

A trifluoromethyl (-CF_3) group (**4k**, -7.133) enhances the docking score, indicating a stronger interaction with CDK-4 compared to a hydrogen atom. Moreover, the presence of chlorine atoms at specific positions (**4l**, -7.326) results in a relatively high docking score, suggesting a positive effect on binding affinity. The introduction of nitro group (**4m**, -7.209) at position-3 contributes to a strong docking score, indicating a favourable interaction with CDK-4. Interestingly, a nitro group at position-4 (**4n**, -7.203) exhibits a docking score similar to **4m**, suggesting that the position of the nitro group does not significantly impact the interaction with CDK-4. The molecular interactions of the compounds with higher docking scores against CDK-4, *viz.* **4e** and **4h** are displayed in Fig. 1b. The docking scores revealed that the chemical nature and position of the substituent groups play a crucial role in determining the binding affinity of the 1,2,4-triazole carboxamide derivatives with both EGFR and CDK-4. These observations provide valuable insights into the structure-activity relationship of these compounds and may

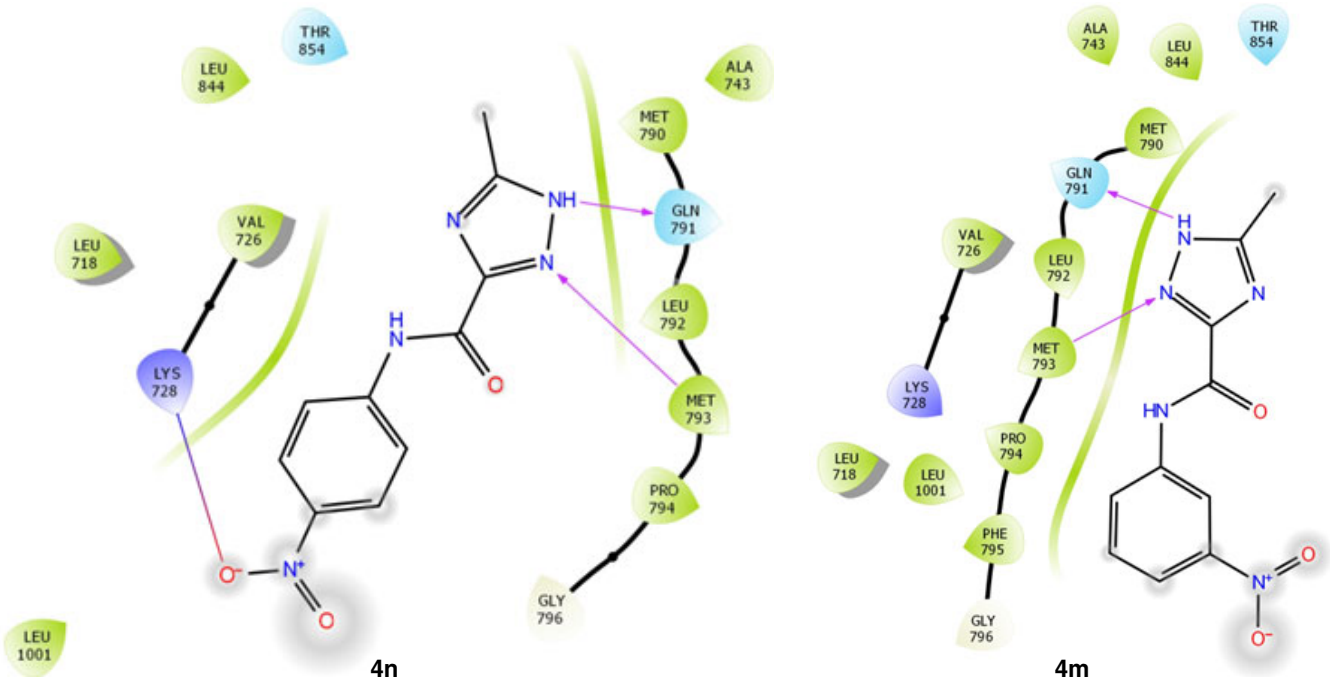

Fig. 1a. Molecular interactions of compounds **4n** and **4m** with EGFR (6LUD) active site

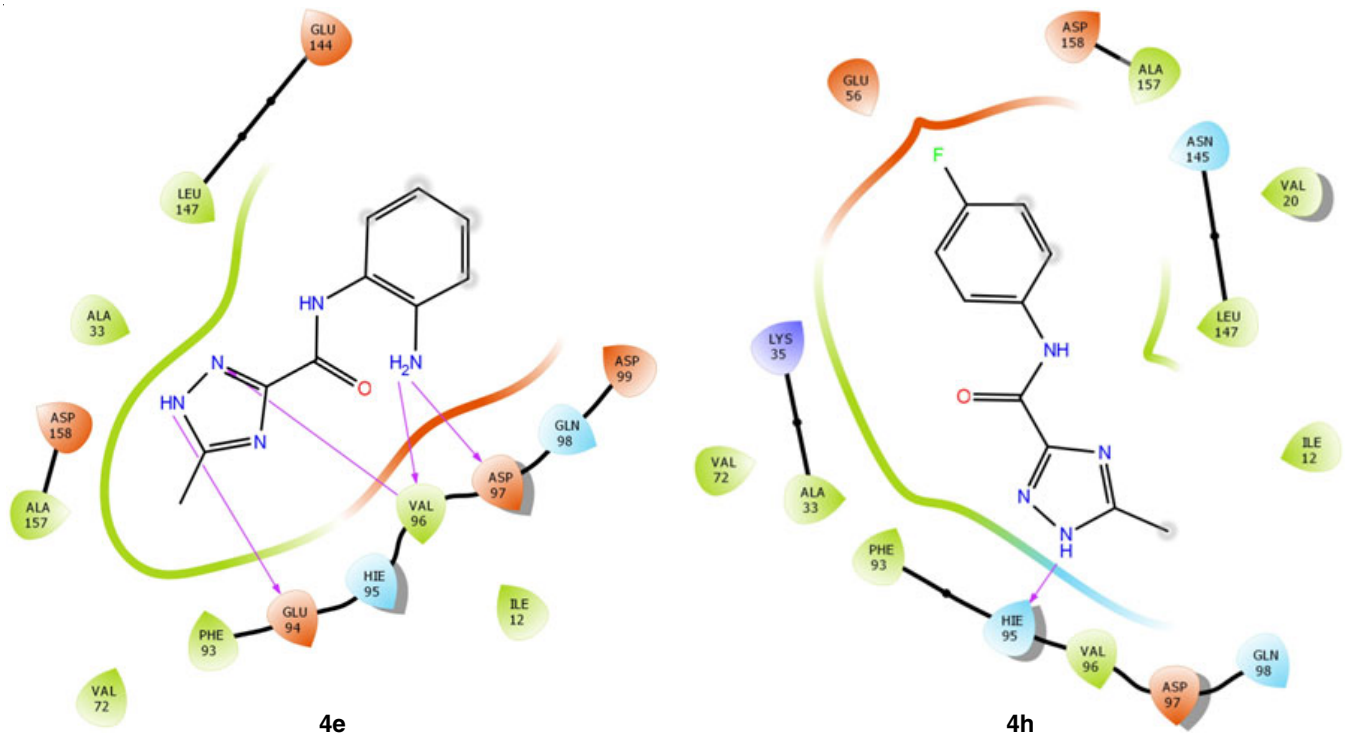

Fig. 1b. Molecular interactions of compounds **4e** and **4h** with CDK-4 (7SJ3) active site

guide further optimization and design of potential drug candidates targeting CDK-4.

Anticancer activity: The MTT assay results for 1,2,4-triazole carboxamide derivatives (**4a-n**) and the reference standard, doxorubicin, in the tested cell lines are given in Table-1. The MTT assay findings indicate that 1,2,4-triazole carboxamide derivatives (**4a-n**) exhibit diverse inhibitory activities in the A-549 non-small cell lung cancer cell line. Among the compounds that were subjected to testing, **4e** (IC_{50} value of 7.11 ± 1.12) and **4m** (IC_{50} value of 6.97 ± 1.12) exhibited the highest levels of inhibitory activity. These compounds displayed IC_{50} values that were significantly lower than that of doxorubicin (IC_{50} value of 1.05 ± 0.95). The aforementioned findings underscore the potential of compounds **4e** and **4m** as viable candidates for subsequent exploration as potent agents in the field of anticancer therapeutics. Several additional compounds (**4a**, IC_{50} = 18.52 ± 2.18; **4c**, IC_{50} = 12.36 ± 0.97; **4d**, IC_{50} = 14.76 ± 2.24; **4h**, IC_{50} = 10 ± 1.18; **4g**, IC_{50} = 18.01 ± 1.12; and **4j**, IC_{50} = 21.72 ± 2.18) demonstrated moderate inhibitory activities in the A-549 cell line, suggesting their potential efficacy. Nevertheless, certain compounds (**4b**, IC_{50} = 25.23 ± 1.58; **4k**, IC_{50} = 26.45 ± 2.74; and **4i**, IC_{50} = 21.34 ± 3.58) exhibited less potent inhibitory effects.

The results of MTT assay for 1,2,4-triazole carboxamide derivatives (**4a-n**) on the colorectal cancer cell line (HCT-116) demonstrate their anticancer properties. Among the tested compounds, compound **4e** (2-NH_2, IC_{50} = 5.11 ± 1.88) is the most potent inhibitor, inhibiting HCT-116 cell proliferation with remarkable efficiency. The inhibitory activity of compound **4m** (3-NO_2, IC_{50} = 10.6 ± 1.25) is comparable to that of compound **4e**, although it is slightly less efficacious. Compounds **4c** (4-CH_3, IC_{50} = 14.21 ± 1.37) and **4d** (4-OCH_3, IC_{50} = 12.61 ± 1.13) exhibit moderate inhibitory activity, inhibiting cell proliferation at relatively low concentrations. In addition, compounds **4f** (4-NH_2, IC_{50} = 17.22 ± 2.23), **4g** (4-OH, IC_{50} = 19.6 ± 1.25) and **4h** (4-F, IC_{50} = 16.71 ± 1.36) inhibit HCT-116 cells with moderate to relatively potent potency. Compounds **4i** (4-Cl, IC_{50} = 24.61 ± 2.39) and **4j** (4-Br, IC_{50} = 19.87 ± 1.56) exhibit significant inhibitory effects as well. In addition, compounds **4a** (H; IC_{50} = 18.71 ± 1.56), **4k** (4-CF_3; IC_{50} = 18.05 ± 3.39) and **4l** (2,4-Cl; IC_{50} = 19.01 ± 1.26) exhibit moderate inhibitory activity. Additionally, compound **4n** (4-NO_2, IC_{50} = 12.71 ± 1.82) demonstrates a moderate inhibitory effect. Comparatively, the IC_{50} value for doxorubicin is 2.39 ± 0.92, indicating its potent inhibitory activity against the HCT-116 cell line.

The results from the MTT assay on the pancreatic cancer cell line (PANC-1) revealed an important information on the inhibitory effects of 1,2,4-triazole carboxamide derivatives (**4a-n**). Compound **4h** (4-F, IC_{50} = 8.32 ± 2.18) stands up as the most potent inhibitor among the investigated compounds, significantly reducing the proliferation of PANC-1 cells. Similarly, compound **4e** (2-NH_2, IC_{50} = 12.3 ± 84.3) shows promising inhibitory efficacy against PANC-1 cells. Compounds **4m** (3-NO_2, IC_{50} = 14.84 ± 2.87) and **4d** (4-OCH_3, IC_{50} = 15.32 ± 1.13) show modest inhibitory effects, demonstrating their potential as inhibitors against PANC-1 cells. Compounds **4c** (4-CH_3), **4f** (4-NH_2) and **4g** (4-OH) similarly show moderate to somewhat robust inhibitory effects (IC_{50} = 15.66 ± 1.95 to 19.51 ± 1.19). To a lesser extent, chemicals **4a** (H, IC_{50} = 28.92 ± 2.78), **4j** (4-Br, IC_{50} = 28.97 ± 1.28) and **4l** (2,4-Cl, IC_{50} = 27.93 ± 1.78) are inhibiting. Compounds **4b** (CH_3), **4k** (4-CF_3) and **4n** (4-NO_2) all display weak inhibitory effects (IC_{50} values of 20.36 ± 3.74 and 16.94 ± 2.78, respectively). Compound **4i** (4-Cl,

IC_{50} = 31.72 ± 3.83) has an IC_{50} value higher than 30 μM, indicating its weaker inhibitory effect.

The MTT assay results for 1,2,4-triazole carboxamide derivatives (**4a-n**) on the cervical cancer cell line (HaLa) indicate their potential as inhibitors against this particular type of cancer. Compound **4f** (4-NH_2, IC_{50} = 20.08 ± 1.34) demonstrates significant inhibitory activity, indicating that it effectively inhibits the growth of HaLa cells. Compound **4i** (4-Cl, IC_{50} = 24.73 ± 4.33), which also exhibits significant inhibitory activity, demonstrates its potential as a potent inhibitor. Compounds **4b** (CH_3, IC_{50} = 23.64 ± 2.94), **4l** (2,4-Cl, IC_{50} = 23.1 ± 3.32) and **4j** (4-Br, IC_{50} = 20.84 ± 1.38) exhibit moderate inhibitory effects, suggesting that they can inhibit the proliferation of HaLa cells. In contrast, among all the tested derivatives, compound **4m** (3-NO_2, IC_{50} = 6.42 ± 1.97) demonstrates the most potent inhibitory activity, with the lowest IC_{50} value. This compound stands out as a promising candidate for further investigation as a potent HaLa cell inhibitor. Compounds **4e** (2-NH_2, IC_{50} = 10.39 ± 1.88), **4h** (4-F, IC_{50} = 11.8 ± 1.32), **4d** (4-OCH_3, IC_{50} = 15.97 ± 1.14) and **4c** (4-CH_3, IC_{50} = 14.08 ± 2.25) display the moderate inhibitory activities, indicating their potential as HaLa cell inhibitors.

The obtained results offer significant insights into the inhibitory potential of these derivatives. All the compounds exhibited minimal cytotoxicity when tested on the normal cell line, specifically the human embryonic kidney cell line (HEK-293). Out of the compounds that were subjected to testing, it was observed that compounds **4e** and **4m** exhibited the highest levels of inhibitory activity. These compounds displayed considerably lower IC_{50} values in comparison to the reference standard, doxorubicin. The aforementioned results underscore the potential of compounds **4e** and **4m** as viable contenders for subsequent exploration as agents with anticancer properties. Moderate to relatively potent inhibitory activities were observed in the A-549, colorectal cancer (HCT-116), pancreatic cancer (PANC-1) and cervical cancer (HaLa) cell lines for various other compounds. Compounds **4c**, **4d**, **4f**, **4g** and **4h** exhibited notable inhibitory effects against diverse cancer cell lines, thereby indicating their potential utility as inhibitors in the context of cancer therapy. In addition, compounds **4a**, **4j** and **4l** exhibited moderate inhibitory activities against various cell lines. Significantly, compound **4e** consistently exhibited notable efficacy in suppressing the proliferation of diverse cancer cell lines, rendering it a particularly auspicious compound for subsequent examination as a potent inhibitor.

Conclusion

A series of novel derivatives of 1,2,4-triazole carboxamides (**4a-n**) were synthesized using a practical multi-step synthetic pathway, resulting in a satisfactory yield for all the synthesized compounds. The results of the molecular docking investigations conducted on the targets EGFR (6LUD) and CDK-4 (7SJ3) demonstrated that the designed compounds exhibited more favourable interactions compared to the ligands that were co-crystallized. The synthesized compounds underwent characterization and subsequent screening to evaluate their potential anticancer activity. This assessment was conducted on four specific cancer cell lines, as well as one normal human cell line. In comparison to the standard drug doxorubicin, the majority of the compounds exhibited notable cytotoxicity potential. The compounds **4e** and **4m** exhibited the highest potency among all the cell lines that were tested. Additional research is required to elucidate the intricate mechanism by which the newly synthesized pyrimidine carboxamide derivatives exert their effects.

CONFLICT OF INTEREST

The authors declare that there is no conflict of interests regarding the publication of this article.

REFERENCES

1. H. Mithoowani and M. Febbraro, *Curr. Oncol.*, **29**, 1828 (2022); https://doi.org/10.3390/curroncol29030150
2. U. Anand, A. Dey, A.K.S. Chandel, R. Sanyal, A. Mishra, D.K. Pandey, V. De Falco, A. Upadhyay, R. Kandimalla, A. Chaudhary, J.K. Dhanjal, S. Dewanjee, J. Vallamkondu and J.M. Pérez de la Lastra, *Genes Dis.*, **10**, 1367 (2023); https://doi.org/10.1016/j.gendis.2022.02.007
3. W.M.C. Van den Boogaard, D.S.J. Komninos and W.P. Vermeij, *Cancers*, **14**, 627 (2022); https://doi.org/10.3390/cancers14030627
4. R. Kaur, A. Ranjan Dwivedi, B. Kumar and V. Kumar, *Anticancer Agents Med. Chem.*, **16**, 465 (2016); https://doi.org/10.2174/1871520615666150819121106
5. E. Bonandi, M.S. Christodoulou, G. Fumagalli, D. Perdicchia, G. Rastelli and D. Passarella, *Drug Discov. Today*, **22**, 1572 (2017); https://doi.org/10.1016/j.drudis.2017.05.014
6. J. Murray, O.E. Young, L. Renshaw, S. White, L. Williams, D.B. Evans, J.S. Thomas, M. Dowsett and J.M. Dixon, *Breast Cancer Res. Treat.*, **114**, 495 (2009); https://doi.org/10.1007/s10549-008-0027-0
7. M.I. Han, H. Bekçi, A.I. Uba, Y. Yildirim, E. Karasulu, A. Cumaoglu, H.Y. Karasulu, K. Yelekçi, O. Yilmaz and S.G. Küçükgüzel, *Arch. Pharm. (Weinheim)*, **352**, 1800365 (2019); https://doi.org/10.1002/ardp.201800365
8. R.Z. Batran, D.H. Dawood, S.A. El-Seginy, M.M. Ali, T.J. Maher, K.S. Gugnani and A.N. Rondon-Ortiz, *Arch. Pharm.*, **350**, 1700064 (2017); https://doi.org/10.1002/ardp.201700064
9. M. Qin, S. Yan, L. Wang, H. Zhang, Y. Zhao, S. Wu, D. Wu and P. Gong, *Eur. J. Med. Chem.*, **115**, 1 (2016); https://doi.org/10.1016/j.ejmech.2016.02.071
10. J. Liu, M. Nie, Y. Wang, J. Hu, F. Zhang, Y. Gao, Y. Liu and P. Gong, *Eur. J. Med. Chem.*, **123**, 431 (2016); https://doi.org/10.1016/j.ejmech.2016.07.059
11. S.A. Shahzad, M. Yar, Z.A. Khan, L. Shahzadi, S.A.R. Naqvi, A. Mahmood, S. Ullah, A.J. Shaikh, T.A. Sherazi, A.T. Bale, J. Kuku³owicz and M. Bajda, *Bioorg. Chem.*, **85**, 209 (2019); https://doi.org/10.1016/j.bioorg.2019.01.005
12. H. Bera, B.J. Tan, L. Sun, A.V. Dolzhenko, W.K. Chui and G.N. Chiu, *Eur. J. Med. Chem.*, **67**, 325 (2013); https://doi.org/10.1016/j.ejmech.2013.06.051
13. I.H. Eissa, A.M. Metwaly, A. Belal, A.B.M. Mehany, R.R. Ayyad, K. El-Adl, H.A. Mahdy, M.S. Taghour, K.M.A. El-Gamal, M.E. El-Sawah, S.A. Elmetwally, M.A. Elhendawy, M.M. Radwan and M.A. ElSohly, *Arch. Pharm.*, **352**, 1900123 (2019); https://doi.org/10.1002/ardp.201900123
14. M.K. Ibrahim, M.S. Taghour, A.M. Metwaly, A. Belal, A.B.M. Mehany, M.A. Elhendawy, M.M. Radwan, A.M. Yassin, N.M. El-Deeb, E.E. Hafez, M.A. ElSohly and I.H. Eissa, *Eur. J. Med. Chem.*, **155**, 117 (2018); https://doi.org/10.1016/j.ejmech.2018.06.004
15. Z. Song, Y. Liu, Z. Dai, W. Liu, K. Zhao, T. Zhang, Y. Hu, X. Zhang and Y. Dai, *Bioorg. Med. Chem.*, **24**, 4723 (2016); https://doi.org/10.1016/j.bmc.2016.08.014

16. G. Sáez-Calvo, A. Sharma, F.A. Balaguer, I. Barasoain, M.Á. Berbís, H. Muñoz-Hernández, J. Rodríguez-Salarichs, N. Olieric, S. Wendeborn, M.A. Peñalva, R. Matesanz, Á. Canales, A.E. Prota, J. Jímenez-Barbero, J.M. Andreu, C. Lamberth, M.O. Steinmetz and J.F. Díaz, *Cell Chem. Biol.*, **24**, 737 (2017); https://doi.org/10.1016/j.chembiol.2017.05.016
17. M. Alswah, A.H. Bayoumi, K. Elgamal, A. Elmorsy, S. Ihmaid and H.E.A. Ahmed, *Molecules*, **23**, 48 (2017); https://doi.org/10.3390/molecules23010048
18. M. Szumilak, A. Wiktorowska-Owczarek and A. Stanczak, *Molecules*, **26**, 2601 (2021); https://doi.org/10.3390/molecules26092601
19. N. Li, C. Chen, H. zhu, Z. Shi, J. Sun and L. Chen, *Bioorg. Chem.*, **111**, 104867 (2021); https://doi.org/10.1016/j.bioorg.2021.104867
20. L.E. Grebenkina, A.V. Matveev and M.V. Chudinov, *Chem. Heterocycl. Compd.*, **56**, 1173 (2020); https://doi.org/10.1007/s10593-020-02794-2
21. J. Park, Y.J. Yoon, B. Kim, H.G. Lee, S.B. Kang, G. Sung, J.J. Kim and S.G. Lee, *Synthesis*, **44**, e1 (2012); https://doi.org/10.1055/s-0031-1289625
22. X.Y. Meng, H.X. Zhang, M. Mezei and M. Cui, *Curr. Computeraided Drug Des.*, **7**, 146 (2011); https://doi.org/10.2174/157340911795677602
23. T.L. Riss, R.A. Moravec, A.L. Niles, S. Duellman, H.A. Benink, T.J. Worzella and L. Minor, Cell Viability Assays - Assay Guidance Manual - NCBI Bookshelf, NCBI Bookshelf (2016).